

Numerical evaluation of QED contribution to lepton $g-2$

T. Aoyama

KMI, Nagoya University

The 33rd International Symposium on Lattice Field Theory
(LATTICE 2015)

July 14–18, 2015, Kobe

Anomalous magnetic moment of lepton

- ▶ Electrons and Muons have magnetic moment along their spins, given by

$$\vec{\mu} = g \frac{e\hbar}{2m} \vec{s}$$

It is known that g -factor deviates from Dirac's value ($g = 2$), and it is called Anomalous magnetic moment

$$a_\ell \equiv (g - 2)/2$$

It is much precisely measured for electron and muon.

- ▶ Electron $g-2$ is explained almost entirely by QED interaction between electron and photons.
It has provided the most stringent test of QED.
- ▶ Muon $g-2$ is more sensitive to high energy physics, and thus a window to new physics beyond the standard model.

10th-order project

- ▶ Numerical evaluation of the entire 10th order QED contribution to lepton $g-2$ has been conducted by the collaboration with:

Toichiro Kinoshita (Cornell, and UMass Amherst)

Makiko Nio (RIKEN)

Masashi Hayakawa (Nagoya University)

Noriaki Watanabe (Nagoya University)

Katsuyuki Asano (Nagoya University)

Electron $g-2$

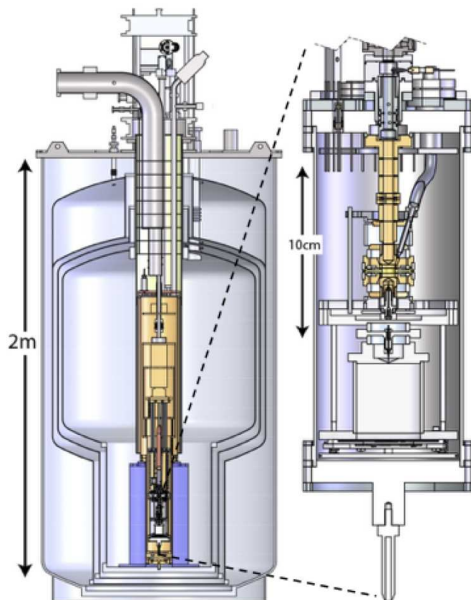


figure from the slide by S. Fogwell Hoogerheide at *Lepton moments 2014*

Anomalous magnetic moment of electron

- ▶ Latest measurement by Harvard group by the resonance of cyclotron and spin levels for a single electron in a cylindrical Penning trap:

$$a_e(\text{HV06}) = 0.001\,159\,652\,180\,85\,(76) \quad [0.66\text{ppb}]$$

Odom, Hanneke, D'Urso, Gabrielse, PRL97, 030801 (2006)

$$a_e(\text{HV08}) = 0.001\,159\,652\,180\,73\,(28) \quad [0.24\text{ppb}]$$

Hanneke, Fogwell, Gabrielse, PRL100, 120801 (2008)

Hanneke, Fogwell Hoogerheide, Gabrielse, PRA83, 052122 (2011)

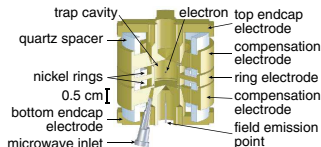


FIG. 2 (color). Cylindrical Penning trap cavity used to confine a single electron and inhibit spontaneous emission.

- ▶ This result is 15-fold improvement over the previous measurement by the University of Washington group:

$$a_{e^-}(\text{UW87}) = 0.001\,159\,652\,188\,4\,(43) \quad [3.7\text{ppb}]$$

$$a_{e^+}(\text{UW87}) = 0.001\,159\,652\,187\,9\,(43) \quad [3.7\text{ppb}]$$

Van Dyck, Schwinger, Dehmelt, PRL59, 26 (1987)

Standard Model prediction of a_e

- ▶ Contributions to electron $g-2$ within the context of the standard model consist of:

$$a_e = a_e(\text{QED}) + a_e(\text{Hadronic}) + a_e(\text{Weak})$$

- ▶ QED contribution can be written as

$$a_e(\text{QED}) = A_1 + \frac{A_2(m_e/m_\mu) + A_2(m_e/m_\tau) + A_3(m_e/m_\mu, m_e/m_\tau)}{\text{mass-dependent contribution}}$$

- ▶ Current status of the standard model prediction is:

$a_e(\text{QED mass-independent})$	0.001 159 652 177 160 (763)
$a_e(\text{QED mass-dependent})$	$2.748 (2) \times 10^{-12}$
$a_e(\text{Hadronic})$	$1.705 (11) \times 10^{-12}$
$a_e(\text{Weak})$	$0.0297 (5) \times 10^{-12}$
<hr/>	
$a_e(\text{theory})$	0.001 159 652 181 643 (763)

* Uncertainty comes from that of fine-structure constant α .

QED contribution

- ▶ QED contributions are evaluated by perturbation theory:

$$a_\ell(\text{QED}) = A^{(2)}\left(\frac{\alpha}{\pi}\right) + A^{(4)}\left(\frac{\alpha}{\pi}\right)^2 + A^{(6)}\left(\frac{\alpha}{\pi}\right)^3 + A^{(8)}\left(\frac{\alpha}{\pi}\right)^4 + \dots$$

- ▶ Up to which order of the QED perturbation theory do we need, to meet the precision of the measurements?

$$\begin{aligned}\left(\frac{\alpha}{\pi}\right)^4 &\simeq 29.1 \times 10^{-12}, \\ \left(\frac{\alpha}{\pi}\right)^5 &\simeq 0.067 \times 10^{-12},\end{aligned}$$

the experimental uncertainty

$$\delta a_e(\text{exp}) = 0.28 \times 10^{-12}.$$

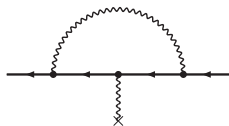
- ▶ Therefore, we need to know $A^{(8)}$ up to $O(10^{-3})$, and $A^{(10)}$ up to $O(10^{-1})$.

QED contribution: 2nd order term

- ▶ 2nd order term comes from 1 Feynman diagram:

$$A_1^{(2)} = \frac{1}{2}$$

Schwinger, PR73, 416 (1948)



- ▶ With this result, the electron $g-2$ up to 2nd order becomes:

$$a_e^{(2)} = 0.001\,161\dots$$

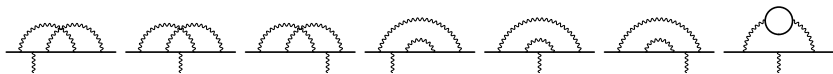
which well explained the observed value in the study of Zeeman splitting of gallium atom by Kusch and Foley in 1947,

$$a_e(\text{KF47}) = 0.001\,19\,(5)$$

Kusch and Foley, PR72, 1256 (1947); PR74, 250 (1948)

QED contribution: 4th order term

- ▶ 4th order term comes from 7 Feynman diagrams:



Their contributions are known analytically:

$$\begin{aligned} A_1^{(4)} &= \frac{197}{144} + \left(\frac{1}{2} - 3 \ln 2 \right) \zeta(2) + \frac{3}{4} \zeta(3) \\ &= -0.328\,478\,965\,579\dots \end{aligned}$$

Petermann, *Helv.Phys.Acta* 30, 407 (1957)
Sommerfield, *PR107*, 328 (1957)

- ▶ 1 diagram with muon or tau-lepton loop also contributes to mass-dependent A_2 terms. Their numerical values are:

$$\begin{aligned} A_2^{(4)}(m_e/m_\mu) &= 5.197\,386\,\underline{67} (26) \times 10^{-7} \\ A_2^{(4)}(m_e/m_\tau) &= 1.837\,98 (34) \times 10^{-9} \end{aligned}$$

Elend, *PL20*, 682 (1966)
Samuel and Li, *PRD44*, 3935 (1991); 46, 4782(E) (1993); Li, Mendel, and Samuel, *PRD47*, 1723 (1993)
Passera, *J.Phys.G31*, R75 (2005)

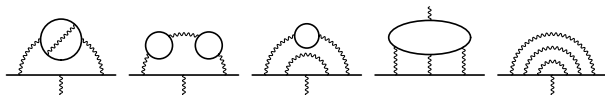
where the values of the mass ratios used are:

$$m_e/m_\mu = 4.836\,331\,66 (12) \times 10^{-3}, \quad m_e/m_\tau = 2.875\,92 (26) \times 10^{-4}.$$

Mohr, Taylor Newell, *Rev.Mod.Phys.*84, 1527 (2012) [CODATA2010]

QED contribution: 6th order term

- ▶ 6th order term receives contributions from 72 Feynman diagrams, represented by these five types:



Their contributions are analytically known, after almost 30 years of works that completed in late 1990's. The numerical values are:

$$A_1^{(6)} = 1.181\,241\,456 \dots$$

$$A_2^{(6)}(m_e/m_\mu) = -0.000\,007\,373\,941\,\underline{62} \quad (27)$$

$$A_2^{(6)}(m_e/m_\tau) = -0.000\,000\,065\,830 \quad (11)$$

$$A_3^{(6)}(m_e/m_\mu, m_e/m_\tau) = 0.000\,000\,000\,000\,190\,\underline{9} \quad (1)$$

Magnaco and Remiddi, Nuovo Cim.A60, 519 (1969)

Barbieri, Remiddi, PLB49, 468 (1974); Barbieri, Caffo, and Remiddi, PLB57, 460 (1975)

Levine, Remiddi, and Roskies, PRD20, 2068 (1979); Laporta and Remiddi, PLB265, 182 (1991); 390, 390 (1995)

Laporta, PRD47, 4793 (1993); PLB343, 421 (1995)

Laporta and Remiddi, PLB379, 283 (1996)

Laporta, Nuovo Cim.A106, 675 (1993); Laporta and Remiddi, PLB301, 440 (1993)

QED contribution: 6th order term

- ▶ Numerical evaluation of these 6th order contributions were started in late 1960's. The early results led to:

$$A_1^{(6)} = 1.195 (26)$$

Kinoshita and Cvitanović, PRD10, 4007 (1974)
cf. Levine and Wright, PRD8, 3171 (1973)

The best numerical value of the diagram M_{6H} combined with the analytical values of the other diagrams was:

$$A_1^{(6)} = 1.181\,259 (40)$$

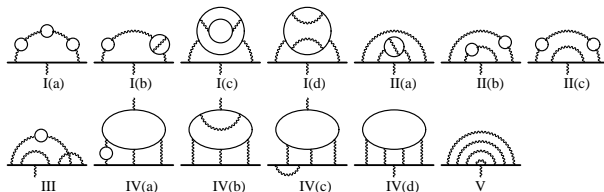
Kinoshita, PRL75, 4728 (1995)

which agrees with the analytical result to 5 digits.

- ▶ Formulation of the numerical evaluation developed for the 6th order calculation has been extended for application to the 8th order, and the present 10th order calculations.

QED contribution: 8th order term

- There are 891 Feynman diagrams contributing to 8th order term. They are classified into 13 gauge-invariant groups.



- They are mostly evaluated by numerical means. The latest result of the mass-independent term $A_1^{(8)}$ is

$$A_1^{(8)} = -1.912 \underline{98} (84)$$

Caffo, Turrini, Remiddi, PRD30, 483 (1984)

Remiddi, Sorella, Lett.Nuovo Cim.44, 231 (1985)

Kinoshita and Lindquist, PRD27, 867 (1983); PRD27, 877 (1987);

PRD27, 886 (1983); PRD39, 2407 (1989); PRD42, 636 (1990)

Kinoshita and Nio, PRL90, 021803 (2003)

Kinoshita and Nio, PRD73, 013003 (2006)

TA, Hayakawa, Kinoshita, Nio, PRL99, 110406 (2007); PRD77, 053012 (2008)

TA, Hayakawa, Kinoshita, Nio, PRL109, 111807 (2012)

TA, Hayakawa, Kinoshita, Nio, PRD91, 033006 (2015)

QED contribution: 8th order term

- ▶ Mass-dependent terms $A_2^{(8)}(m_e/m_\mu)$, $A_2^{(8)}(m_e/m_\tau)$, and $A_3^{(8)}(m_e/m_\mu, m_e/m_\tau)$ are also evaluated numerically:

$$A_2^{(8)}(m_e/m_\mu) = 0.000\ 922\ \underline{66}$$

$$A_2^{(8)}(m_e/m_\tau) = 0.000\ 008\ \underline{24}\ (12)$$

$$\rightarrow 0.000\ 007\ \underline{38}\ (12)^*$$

$$A_3^{(8)}(m_e/m_\mu, m_e/m_\tau) = 0.000\ 000\ \underline{746\ 5}\ (18)$$

TA, Hayakawa, Kinoshita, Nio, PRL109, 111807 (2012)

(* after correcting the typo found in the literature)

- ▶ Recently these terms were evaluated by analytic method in heavy lepton-mass expansion.

$$A_2^{(8)}(m_e/m_\mu) = 0.000\ 916\ 197\ \underline{070\ 3}\ (373)$$

$$A_2^{(8)}(m_e/m_\tau) = 0.000\ 007\ \underline{429\ 24}\ (118)$$

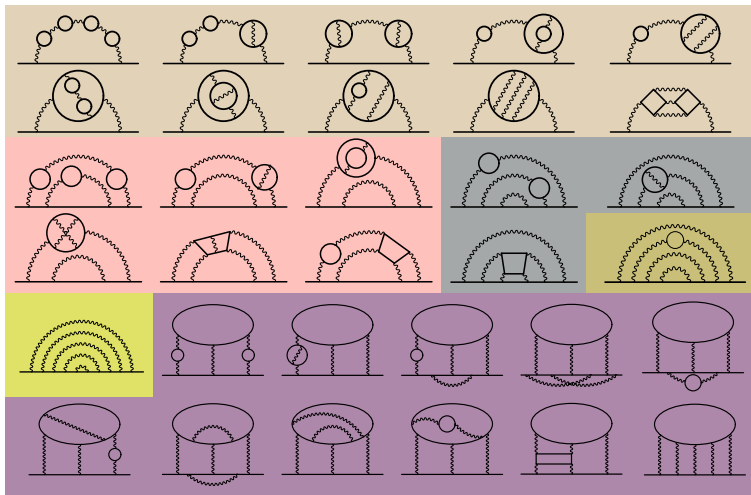
$$A_3^{(8)}(m_e/m_\mu, m_e/m_\tau) = 0.000\ 000\ \underline{746\ 87}\ (28)$$

Kurz, Liu, Marquard, Steinhauser, NPB879, 1 (2014)

The agreement of these two values confirmed our numerical results.

QED contribution: 10th order term

- ▶ 12 672 Feynman diagrams contribute to 10th order term.
They are classified into 32 gauge invariant sets within 6 supersets.



QED contribution: 10th order term

- ▶ Numerical evaluation of the complete 10th order contribution was reported in 2012 and an updated result was published in 2015.

$$A_1^{(10)} = 7.795 \underline{(336)}$$

Kinoshita and Nio, PRD73, 053007 (2006)

TA, Hayakawa, Kinoshita, Nio, Watanabe, PRD78, 053005 (2008)

TA, Asano, Hayakawa, Kinoshita, Nio, Watanabe, PRD81, 053009 (2010)

TA, Hayakawa, Kinoshita, Nio, PRD78, 113006 (2008); 82, 113004 (2010); 83, 053002 (2011)

83, 053003 (2011); 84, 053003 (2011); 85, 033007 (2012); 85, 093013 (2012)

TA, Hayakawa, Kinoshita, Nio, PRL109, 111807 (2012); PRD91, 033006 (2015)

- ▶ Contribution to $A_1^{(10)}$ mainly comes from Set V that consists of 6354 vertex diagrams without closed lepton loops.
- ▶ Mass-dependent term is also evaluated:

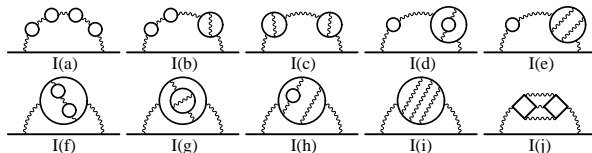
$$A_2^{(10)}(m_e/m_\mu) = -0.003 \underline{82} \text{ (39)}$$

tau-lepton contribution is negligibly small for the current experimental precision.

QED contribution: 10th order term

- Recently, Set I that consists of 208 diagrams are evaluated (semi-) analytically for mass-dependent and mass-independent contributions.

Baikov, Maier, Marquard, NPB877, 647 (2013)

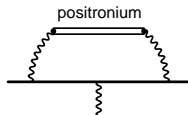


- Their results of $A_1^{(10)}$ [Set I] are consistent with our numerical evaluations:

	Baikov et al.	AHKN, PRL2012
I(a)	0.000 471	0.000 470 94 (6)
I(b)	0.007 010	0.007 010 8 (7)
I(c)	0.023 467	0.023 468 (2)
I(d) + I(e)	0.014 094	0.014 098 (5)(4)
I(e)	0.010 291	0.010 296 (4)
I(f) + I(g) + I(h)	0.037 85 ⁺⁵ ₋₃	0.037 833 (20)(6)(13)
I(i)	0.017 21 ⁺⁸ ₋₂₃	0.017 47 (11)
		→ 0.017 324 (12) (updated)
I(j)	0.000 420 ⁺³¹ ₋₁₆	0.000 397 5 (18)

Positronium contribution?

- ▶ Recently it was addressed that positronium pole gives rise to extra contribution to the vacuum-polarization loop at order α^5 .



Mishima, arXiv:1311.7109
Fael and Passera, PRD90, 056004 (2014)

- ▶ It was claimed that the positronium contributes through a specific class of diagram of $O(\alpha^7)$.

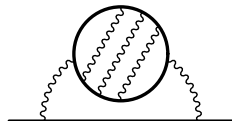
Hayakawa, arXiv:1403.0416

- ▶ It turns out that one-half of this effect is cancelled by the e^-e^+ scattering contribution near threshold, and the remaining half is included in the perturbative calculation of the 10th-order diagram Set I(i).

Melnikov, Vainshtein, and Voloshin, PRD90, 017301 (2014); Eides, PRD90, 057301 (2014)
Fael and Passera, PRD90, 056004 (2014)

Braun, Zh.Eksp.Teor.Fiz 54, 1220 (1968); Barbieri, Christillin, and Remiddi, PRA8, 2266 (1973)

- ▶ Thus, no additional contribution beyond the perturbative calculation is present.



Set I(i)

Hadronic and electroweak contributions

- ▶ Hadronic contribution is mostly derived from experimental data related to hadronic vacuum polarization. We quote the recent evaluations up to next-to-next-to-leading order that lead to:

$$a_e(\text{had. v.p.}) = 1.866 (10)_{\text{exp}(5)}_{\text{rad}} \times 10^{-12}$$

$$a_e(\text{had. v.p. NLO}) = -0.223 4 (12)_{\text{exp}(7)}_{\text{rad}} \times 10^{-12}$$

$$a_e(\text{had. v.p. NNLO}) = 0.028 (1) \times 10^{-12}$$

Nomura and Teubner, NPB867, 236 (2013)

Kurz, Liu, Marquard, and Steinhauser, PLB734, 144 (2014)

The hadronic light-by-light-scattering (l-by-l) term is given by:

$$a_e(\text{had. l-by-l}) = 0.035 (10) \times 10^{-12}$$

Prades, de Rafael, and Vainshtein, in *Lepton Dipole Moments* (2009)

- ▶ Electroweak contribution has been obtained from the analytic form up to two-loop effect on the muon $g-2$ adapted for the electron.

$$a_e(\text{weak}) = 0.029 7 (5) \times 10^{-12}$$

Fujikawa, Lee, and Sanda, PRD6, 2923 (1972)

Czarnecki, Krause, and Marciano, PRL76, 3267 (1996)

Knecht, Peris, Perrottet, and de Rafael, JHEP11, 003 (2002)

Czarnecki, Marciano, and Vainshtein, PRD67, 073006 (2003); 73, 119901(E) (2006)

- ▶ These contributions are small but non-negligible.

Standard model prediction

- ▶ Thus, the theoretical prediction of electron $g-2$ is given by:

$$a_e(\text{theory}) = a_e(\text{QED}) + a_e(\text{hadronic}) + a_e(\text{weak})$$

where

$$a_e(\text{QED}) = 0.5 \left(\frac{\alpha}{\pi} \right) \quad (\text{exact})$$

$$- 0.328\,478\,444\,002\,\underline{55} \text{ (22)} \left(\frac{\alpha}{\pi} \right)^2 \quad O(10^{-18})$$

$$+ 1.181\,234\,016\,8\underline{16} \text{ (11)} \left(\frac{\alpha}{\pi} \right)^3 \quad O(10^{-19})$$

$$- 1.912\,\underline{06} \text{ (84)} \left(\frac{\alpha}{\pi} \right)^4 \quad 0.25 \times 10^{-13}$$

$$+ 7.\underline{791} \text{ (336)} \left(\frac{\alpha}{\pi} \right)^5 \quad 0.23 \times 10^{-13}$$

$$a_e(\text{hadronic}) = 1.7\underline{056} \text{ (151)} \times 10^{-12} \quad 0.16 \times 10^{-13}$$

$$a_e(\text{weak}) = 0.029 \underline{7} \text{ (5)} \times 10^{-12} \quad O(10^{-15})$$

Input values to theoretical prediction

- ▶ To compare the theoretical prediction with the experiment, the value of the fine structure constant α is needed which is determined by an independent method.
- ▶ The best value of such α has been obtained from the determination of h/m_{Rb} by the measurement of recoil velocity of ^{87}Rb , through the relation:

$$\alpha = \left[\frac{2R_{\infty}}{c} \frac{m_{\text{Rb}}}{m_e} \frac{h}{m_{\text{Rb}}} \right]^{1/2}$$

where

$$h/m_{\text{Rb}} = 4.591\,359\,272\,9\,(57) \times 10^{-9} \text{ m}^2\text{s}^{-1} \quad [1.2 \times 10^{-9}]$$

$$c = 299\,792\,458 \text{ ms}^{-1} \quad (\text{exact})$$

$$R_{\infty} = 10\,973\,731.568\,539\,(55) \text{ m}^{-1} \quad [5.0 \times 10^{-12}]$$

$$m_e = 0.000\,548\,579\,909\,46\,(22) \text{ amu} \quad [4.0 \times 10^{-10}]$$

$$m_{\text{Rb}} = 86.909\,180\,535\,(10) \text{ amu} \quad [1.2 \times 10^{-10}]$$

Bouchendira, Cladé, Guellati-Khélifa, Nez, and Biraben, PRL 106, 080801 (2011)

Mohr, Taylor, and Newell, RMP84, 1527 (2012) [CODATA2010]

Mount, Redshaw, and Myers, PRA82, 042513 (2010)

It leads to

$$\alpha^{-1}(\text{Rb}) = 137.035\,999\,037\,(91) \quad [0.66 \times 10^{-9}]$$

Theoretical prediction of electron $g-2$

- ▶ With this α , the theoretical prediction of a_e becomes:

$$a_e(\text{theory}) = 1\,159\,652\,181.643\ (25)(23)(16)(763) \times 10^{-12}$$

(8th)(10th)(had+ew)(α)

uncertainty comes from QED 8th order term, 10th order term, hadronic+electroweak, and uncertainty of α (Rb).

- ▶ It is in good agreement with the experiment:

$$a_e(\text{exp}) = 1\,159\,652\,180.73\ (28) \times 10^{-12}$$

Hanneke, Fogwell, Gabrielse, PRL 100, 120801 (2008)

The difference is:

$$a_e(\text{exp}) - a_e(\text{theory}) = -0.91\ (82) \times 10^{-12}$$

Fine Structure Constant α

- From the measurement and the theory of electron $g-2$, the value of fine-structure constant can be determined.

Experimental value $\rightarrow a_e = A^{(2)} \left(\frac{\alpha}{\pi}\right) + A^{(4)} \left(\frac{\alpha}{\pi}\right)^2 + A^{(6)} \left(\frac{\alpha}{\pi}\right)^3 + A^{(8)} \left(\frac{\alpha}{\pi}\right)^4 + A^{(10)} \left(\frac{\alpha}{\pi}\right)^5 + \dots$

Theoretical calculations \rightarrow (arrows pointing to the terms in the series)

+(small contributions)

$\alpha^4 \alpha^5$ had+ew exp
(29) (27) (18) (331)

- Newly obtained value of fine-structure constant is:

$$\alpha^{-1}(a_e) = 137.035\,999\,1570\,(334) \quad [0.25\text{ppb}]$$

TA, Hayakawa, Kinoshita, Nio, Phys. Rev. D 91, 033006 (2015)

c.f.

$$\alpha^{-1}(\text{Rb}) = 137.035\,999\,037\,(91) \quad [0.66\text{ppb}]$$

Bouchendira *et al.*, PRL 106, 080801 (2011)

$$\alpha^{-1}(\text{Cs}) = 137.036\,000\,00\,(110) \quad [8.0\text{ppb}]$$

Wicht, *et al.*, Phys. Scr. T102, 82 (2002)
Gerginov, *et al.*, PRA 73, 032504 (2006)

Muon $g-2$

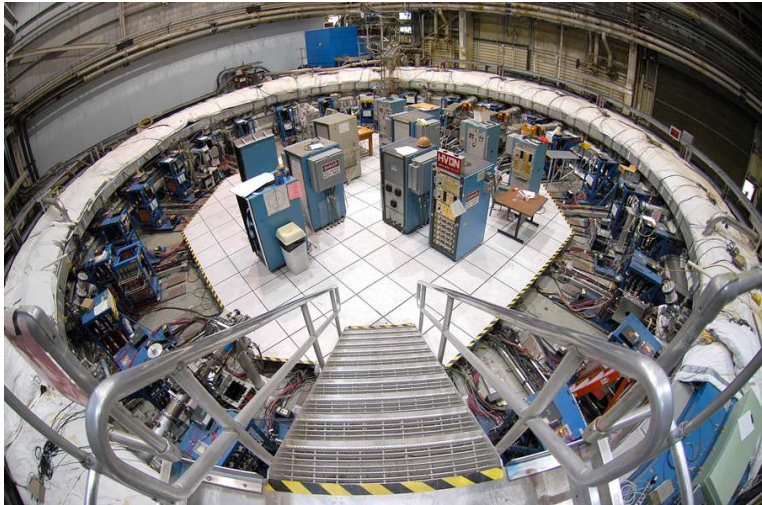
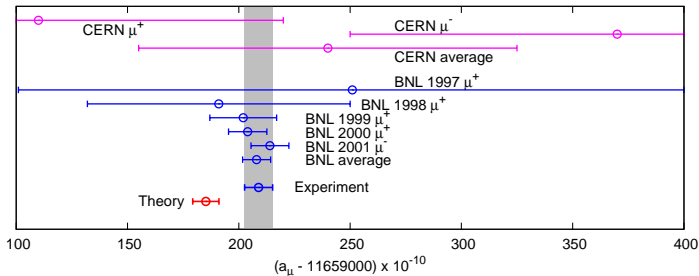


photo from BNL

Muon $g-2$: experiment

- ▶ The anomalous magnetic moment of muon has also been studied extensively in both experiment and theory.
- ▶ Experiments using muon storage ring started at CERN in 1960's. The latest experiment was conducted at BNL in E821 experiment.



- ▶ Latest world average of the measured a_μ :

$$a_\mu[\text{exp}] = 116\,592\,089\,(63) \times 10^{-11} \quad [0.54\text{ppm}]$$

Bennett, et al., Phys. Rev. D73, 072003 (2006)
Roberts, Chinese Phys. C 34, 741 (2010)

Muon $g-2$: theory

- ▶ Contributions to muon $g-2$ may be expressed as:

$$a_\mu = a_\mu(\text{QED}) + a_\mu(\text{hadronic}) + a_\mu(\text{weak})$$

where

$$a_\mu(\text{QED}) = \underbrace{A_1}_{\text{mass-independent contribution}} + \underbrace{A_2(m_\mu/m_e) + A_2(m_\mu/m_\tau) + A_3(m_\mu/m_e, m_\mu/m_\tau)}_{\text{mass-dependent contribution}}$$

mass-independent contribution
universal to electron and muon

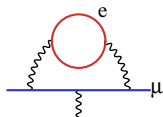
- ▶ QED contributions are evaluated by perturbation theory:

$$A_i = A_i^{(2)} \left(\frac{\alpha}{\pi}\right) + A_i^{(4)} \left(\frac{\alpha}{\pi}\right)^2 + A_i^{(6)} \left(\frac{\alpha}{\pi}\right)^3 + \dots, \quad i = 1, 2, 3$$

QED contribution

- ▶ What distinguishes $a_e(\text{QED})$ and $a_\mu(\text{QED})$ is the mass-dependent component.
- ▶ Light lepton loop contribution yields large logarithmic enhancement involving a factor $\ln(m_e/m_\mu)$.
 - ▶ Vacuum polarization loop:

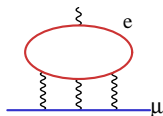
$$\frac{2}{3} \ln(m_\mu/m_e) - \frac{5}{9} \simeq 3.$$



- ▶ Light-by-light scattering loop:

$$\frac{2}{3} \pi^2 \ln(m_\mu/m_e) \simeq 35.$$

6th-order l-by-l effect is important.



c.f. Aldins, Kinoshita, Brodsky, Dufner, PRL8, 441 (1969)

- ▶ Therefore, the sets of diagrams giving the leading contribution can be identified and were evaluated in the earlier stage.
The entire contribution including non-leading diagrams have been evaluated.

QED contribution

- ▶ $a_\mu(\text{QED})$ is known up to 10th order. Their values contributing to mass-dependent terms are:

	$A_2(m_\mu/m_e)$	$A_2(m_\mu/m_\tau)$	$A_3(m_\mu/m_e, m_\mu/m_\tau)$
4th	1.094 258 3120 (83)	0.000 078 079 (15)	—
6th	22.868 380 04 (23)	0.000 360 70 (13)	0.000 527 76 (11)
8th	132.685 2 (60)	0.042 941 (2)(53)	0.062 72 (4)
10th	742.18 (87)	-0.068 (5)	2.011 (10)

Samuel and Li, PRD44, 3935 (1991); Li, Mendel and Samuel, PRD47, 1723 (1993)
 Laporta, Nuovo Cim. A106, 675 (1993); Laporta and Remiddi, PLB301, 440 (1993); Czarnecki and Skrzypek, PLB449, 354 (1999)
 Laporta, PLB312, 495 (1993); Kinoshita and Nio, PRD70, 113001 (2004); Kurz, Liu, Marquard, Steinhauser, NPB879, 1 (2014)
 Laporta, PLB328, 522 (1994); Kinoshita and Nio, PRD73, 053007 (2006)
 TA, Hayakawa, Kinoshita, Nio, Watanabe, PRD78, 053005 (2008)
 TA, Asano, Hayakawa, Kinoshita, Nio, Watanabe, PRD81, 053009 (2010)
 TA, Hayakawa, Kinoshita, Nio, PRD78, 113006 (2008); 82, 113004 (2010); 83, 053002 (2011)
 83, 053003 (2011); 84, 053003 (2011); 85, 033007 (2012); 85, 093013 (2012)

- ▶ Together with the mass-independent term A_1 , we obtain:

$$a_\mu(\text{QED}) = 116\,584\,718.935\,(9)\,(18)\,(7)\,(77) \times 10^{-11}$$

(mass ratio)(8th)(10th)($\alpha(\text{Rb})$)

Hadronic and electroweak contributions

- Recent evaluations of the hadronic vacuum polarization contributions and the hadronic light-by-light-scattering (l-by-l) terms are given by:

$$a_\mu(\text{had. v.p.}) = 6949.1 (37.2)_{\text{exp}}(21.0)_{\text{rad}} \times 10^{-11}$$

$$a_\mu(\text{had. v.p. NLO}) = -98.4 (0.6)_{\text{exp}}(0.4)_{\text{rad}} \times 10^{-11}$$

$$a_\mu(\text{had. v.p. NNLO}) = 12.4 (0.1) \times 10^{-11}$$

$$a_\mu(\text{had. l-by-l}) = 116 (40) \times 10^{-11}$$

$$a_\mu(\text{had. l-by-l NLO}) = 3 (2) \times 10^{-11}$$

Hagiwara, Liao, Martin, Nomura, Teubner, J.Phys.G38, 085003 (2011)

Kurz, Liu, Marquard, and Steinhauser, PLB734, 144 (2014)

Prades, de Rafael, and Vainshtein, in *Lepton Dipole Moments* (2009)

Colangelo, Hoferichter, Nyffeler, Passera, Stoffer, PLB735, 90 (2014)

- Electroweak contribution has been evaluated up to 2-loop order:

$$a_\mu(\text{weak}) = 154 (2) \times 10^{-11}$$

Fujikawa, Lee, and Sanda, PRD6, 2923 (1972)

Czarnecki, Krause, and Marciano, PRL76, 3267 (1996)

Knecht, Peris, Perrotet, and de Rafael, JHEP11, 003 (2002)

Czarnecki, Marciano, and Vainshtein, PRD67, 073006 (2003); 73, 119901(E) (2006)

Muon $g-2$: comparison with experiment

- ▶ The theoretical value of a_μ in the standard model is given by:

$$a_\mu(\text{theory}) = 116\,591\,855.03 \text{ (0.08) (58.56) (2)} \times 10^{-11}$$

(QED)(hadronic)(weak)

- ▶ Comparing the theoretical result with the experimental value, we obtain:

$$a_\mu(\text{BNL06}) - a_\mu(\text{theory}) = 234 \text{ (87)} \times 10^{-11} \quad [2.7\sigma]$$

- ▶ It is an urgent problem to understand whether this 2.7σ discrepancy between experiment and theory is real.
- ▶ If the discrepancy still persists in the future improvement of both measurement and theory, it may be regarded as an indication of new physics beyond the standard model.
- ▶ By the complete evaluation of QED 10th order contribution, the QED part has been pinned down precisely for the next experiments. It enables us to concentrate on improving the precision of the hadronic part.

Muon $g-2$: future experiment

- ▶ New experiments are being prepared:

- ▶ Fermilab P989 experiment using BNL muon storage ring.

B. L. Roberts (Fermilab P989 Collaboration), Nucl. Phys. B Proc. Suppl. 218, 237 (2011)

- ▶ J-PARC using ultra-cold muon beam

H. Iinuma (J-PARC New $g-2$ /EDM Experiment Collaboration), J. Phys. Conf. Ser. 295, 012032 (2011).

Both aim at $\sim 0.1\text{ppm}$ (12×10^{-11}) level of uncertainty.



photo from Fermilab

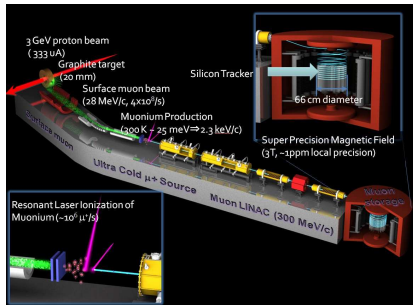


image from KEK

Numerical evaluation

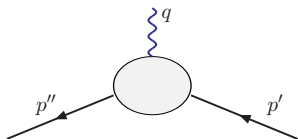


Formulation

- ▶ Magnetic property of lepton can be studied through examining its scattering by a static magnetic field.

The amplitude can be represented as:

$$e\bar{u}(p'') \left[\gamma^\mu F_1(q^2) + \frac{i}{2m} \sigma^{\mu\nu} q_\nu F_2(q^2) \right] u(p') A_\mu^e(\vec{q})$$



- ▶ The anomalous magnetic moment is the static limit of the magnetic form factor $F_2(q^2)$:

$$a_\ell = F_2(0) = Z_2 M, \quad M = \lim_{q^2 \rightarrow 0} \text{Tr}(P_\nu(p, q)\Gamma^\nu)$$

where Γ^ν is the proper vertex function with the external lepton on the mass shell, and $P_\nu(p, q)$ is the magnetic projection operator.

Numerical Approach



- ▶ In the following, let us focus on the set of diagrams without lepton loops, called q -type:
 - ▶ 518 of 891 diagrams contributing to 8th order $A_1^{(8)}$ term (Group V),
 - ▶ 6354 of 12,672 diagrams contributing to 10th order $A_1^{(10)}$ term (Set V).

Other sets of diagrams are treated in a similar way.

Numerical Approach

► Procedure:

- Step 1.** Find distinct set of Feynman diagrams.
- Step 2.** Construct **amplitude** in terms of Feynman parametric integral.
- Step 3.** Construct subtraction terms of **UV divergence**.
 - *K*-operation
- Step 4.** Construct subtraction terms of **IR divergence**.
 - *R*-subtraction of residual mass-renormalization.
 - *I*-subtraction of logarithmic IR divergences.
- Step 5.** Evaluate the finite amplitude by numerical integration.
- Step 6.** Carry out **residual renormalization** to achieve the standard on-shell renormalization.

Diagrams

- ▶ Combined uncertainty of contributions from N diagrams grows roughly as \sqrt{N} . Thus it is important to reduce the number of independent integrals.
- ▶ A set of vertex diagrams Λ obtained by inserting an external vertex into each lepton line of self-energy diagram Σ can be related by Ward-Takahashi identity.

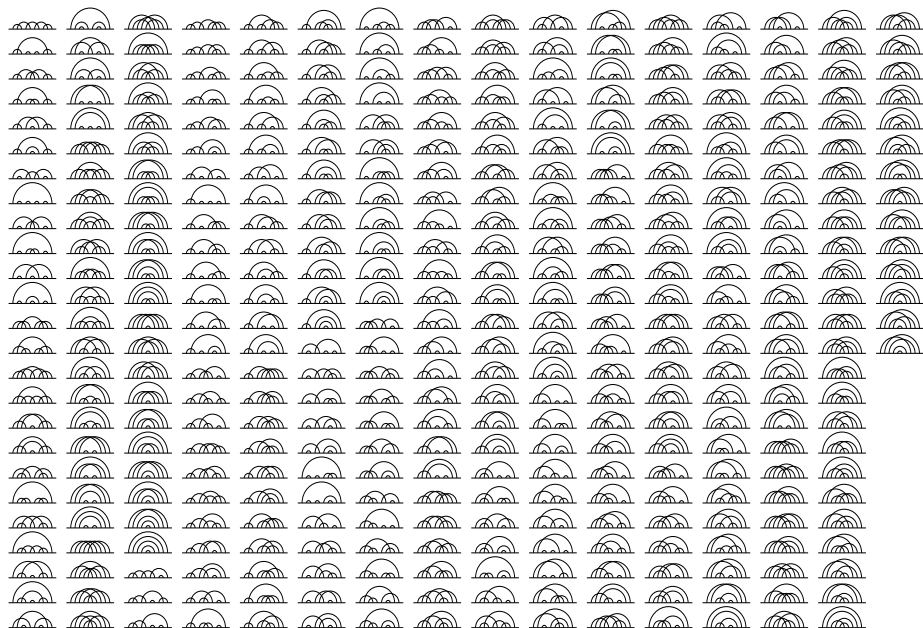
$$\Lambda^\nu(p, q) \simeq -q_\mu \left. \frac{\partial \Lambda^\mu(p, q)}{\partial q_\nu} \right|_{q \rightarrow 0} - \frac{\partial \Sigma(p)}{\partial p_\nu}.$$

e.g. 4th-order case:



- ▶ For Set V diagrams, the number of independent integrals goes from **6354** to **706** by WT sum, further reduced by time-reversal symmetry to **389**.

Diagrams: 389 independent integrals for 10th-order Set V

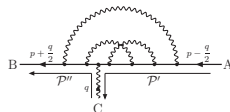
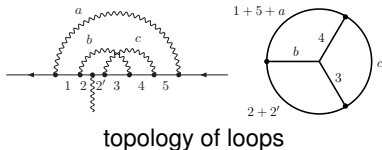


Construction of Amplitude

- ▶ Amplitude is given by an integral over loop momenta according to Feynman-Dyson rule.
- ▶ It is converted into Feynman parametric integral over $\{z_i\}$. Momentum integration is carried out analytically that yields

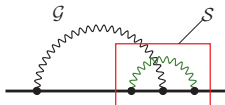
$$M_G^{(2n)} = \left(-\frac{1}{4}\right)^n \Gamma(n-1) \int (dz)_G \left[\frac{F_0}{U^2 V^{n-1}} + \frac{F_1}{U^3 V^{n-2}} + \dots \right]$$

- ▶ Integrand is expressed by a rational function of terms called *building blocks*, U , V , B_{ij} , A_j , and C_{ij} .
- ▶ Building blocks are given by functions of $\{z_i\}$, reflecting the topology of diagram, flow of momenta, etc.



Subtraction of UV Divergences

- ▶ UV divergence occurs when loop momenta in a subdiagram go to infinity. It corresponds to the region of Feynman parameter space $z_i \sim \mathcal{O}(\epsilon)$ for $i \in S$.



- ▶ In order to carry out subtraction numerically, the singularities are cancelled point-by-point on Feynman parameter space.

$$M_G - L_S M_{G/S} \longrightarrow \int (dz)_G \left[m_G - \mathbb{K}_S m_G \right]$$

- ▶ The subtraction integrand $\mathbb{K}_S m_G$ is derived from m_G by simple power-counting rule called ***K-operation***. Cvitanović and Kinoshita, 1974
- ▶ By construction, subtraction terms can be factorized into (UV-divergent part of) renormalization constant and lower-order magnetic part.

$$\int (dz)_G \left[\mathbb{K}_S m_G \right] = L_S^{\text{UV}} M_{G/S}$$

L_S^{UV} is the leading UV-divergent part of L_S . The difference $(L_S^{\text{UV}} - L_S)$ must be adjusted in later step called **residual renormalization**.

Subtraction of UV divergence

- ▶ K-operation yields UV subtraction terms corresponding to divergent subdiagram S :

- ▶ for a vertex subdiagram,

$$\mathbb{K}_S M_G = L_S^{\text{UV}} M_{G/S}$$

where L_S^{UV} is divergent part of vertex renormalization constant.

- ▶ for a self-energy subdiagram,

$$\mathbb{K}_S M_G = \delta m_S^{\text{UV}} M_{G/S(i^*)} + B_S^{\text{UV}} M_{G/[S,i]}$$

where δm_S^{UV} and B_S^{UV} are divergent parts of mass and wave-function renormalization constants.

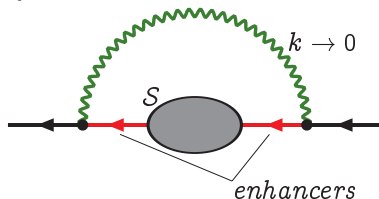
- ▶ When there are more than one divergent subdiagram, all subdivergences are identified by Zimmermann's forest formula. UV-finite amplitude M_G^{R} is given by

$$M_G^{\text{R}} = M_G + \sum_f \prod_{S \in f} (-\mathbb{K}_S) M_G$$

where a forest f is a set of divergent subdiagrams without partial-overlapping.

IR subtraction Scheme

- ▶ A diagram may have IR divergence when some momenta of photon go to zero. It is really divergent by “enhancer” leptons that are close to on-shell by kinematical constraint.



- ▶ We adopt subtraction approach for these divergences point-by-point on Feynman parameter space.
- ▶ There are two types of sources of IR divergence in M_G associated with a self-energy subdiagram. To handle these divergences, we introduce two subtraction operations:

- ▶ **R-subtraction** to remove the residual self-mass term

$$\mathbb{R}_S M_G = \widetilde{\delta m}_S M_{G/S(i^*)}$$

- ▶ **I-subtraction** to subtract remaining logarithmic IR divergence

$$\mathbb{I}_S M_G = \widetilde{L}_{G/S(k)} M_S$$

Nested IR singularities

- ▶ Nested IR divergences emerge when there are more than one self-energy subdiagram account for IR singularity.
- ▶ These divergences are dealt with the combination of I-/R-subtractions, conducted in a forest-like structure, which we call

“annotated forests”.

a forest with the annotation that each subdiagram in the forest accounts to either of I- and R-subtractions.

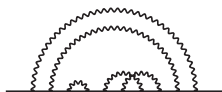
- ▶ IR-finite amplitude ΔM_G is given by

$$\Delta M_G = \sum_{\tilde{f}} (-\mathbb{I}_{S_j}) \cdots (-\mathbb{R}_{S_k}) \cdots M_G^R$$

where $S_j, S_k \in \tilde{f}$: annotated forest.

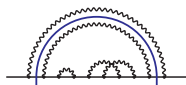
Subtraction terms: Example

- ▶ Consider a 10th-order diagram $M_{X_{253}}$:

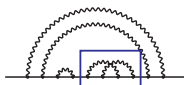


- ▶ $M_{X_{253}}$ have

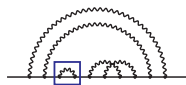
- three self-energy subdiagrams (S_1, S_2, S_3),



S_1

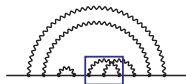


S_2

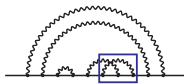


S_3

- two vertex subdiagrams (S_4, S_5).



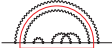
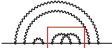

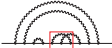
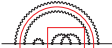
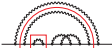
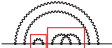

S_4



S_5

UV Forests












- According to Zimmermann's forest formula, 23 UV divergent parts and corresponding subtraction terms are identified as:

forest	subtraction	expression	
	$\{S_1\}$	\mathbb{K}_{28}	$-dm_{16}^{UV} M_{2^*} - B_{16}^{UV} M_2$
	$\{S_2\}$	\mathbb{K}_{57}	$-dm_{4a}^{UV} M_{6b(2^*)} - B_{4a}^{UV} M_{6b}$
	$\{S_3\}$	\mathbb{K}_{33}	$-dm_2 M_{42(2^*)} - B_2^{UV} M_{42}$
	$\{S_4\}$	\mathbb{K}_{56}	$-L_2^{UV} M_{30}$
	$\{S_1, S_2\}$	$\mathbb{K}_{28}\mathbb{K}_{57}$	$+dm_{4a}^{UV} dm_{4b(1^*)}^{UV} M_{2^*} + B_{4a}^{UV} dm_{4b}^{UV} M_{2^*} + B_{4a}^{UV} B_{4b}^{UV} M_2$
	$\{S_1, S_3\}$	$\mathbb{K}_{28}\mathbb{K}_{33}$	$+dm_2 dm_{6c(1^*)}^{UV} M_{2^*} + B_2^{UV} dm_{6c}^{UV} M_{2^*} + B_2^{UV} B_{6c}^{UV} M_2$
	$\{S_2, S_3\}$	$\mathbb{K}_{33}\mathbb{K}_{57}$	$+dm_2 dm_{4a}^{UV} M_{4b(2^{**})} + dm_2 B_{4a}^{UV} M_{4b(2^*)} + B_2^{UV} dm_{4a}^{UV} M_{4b(2^*)} + B_2^{UV} B_{4a}^{UV} M_{4b}$
	$\{S_1, S_2, S_3\}$	$\mathbb{K}_{28}\mathbb{K}_{33}\mathbb{K}_{57}$	$-dm_2 dm_{4a}^{UV} dm_{2^{**}}^{UV} M_{2^*} - dm_2 B_{4a}^{UV} dm_{2^*}^{UV} M_{2^*} - B_2^{UV} dm_{4a}^{UV} dm_{2^*}^{UV} M_{2^*} - B_2^{UV} B_{4a}^{UV} dm_2 M_{2^*} - B_2^{UV} B_{4a}^{UV} B_2^{UV} M_2$

and 15 other forests involving either S_4 or S_5 .

“Annotated forests” for IR subtraction

- 11 IR subtraction terms are identified by combination of self-energy type subdiagrams with distinction of I - or R -subtraction operation as:

	annotation	subtraction	expression
	$G \rightarrow M, S_1 \rightarrow dm$	\mathbb{R}_{2-8}	$-dm_{16}^R M_{2*}$
	$G \rightarrow M, S_2 \rightarrow dm$	\mathbb{R}_{567}	$-dm_{4a}^R M_{6b(2*)}^R$
	$G \rightarrow M, S_1 \rightarrow dm, S_2 \rightarrow dm$	$\mathbb{R}_{2-8} \mathbb{R}_{567}$	$+dm_{4a}^R dm_{4b(1*)}^R M_{2*}$
	$G \rightarrow I, S_1 \rightarrow M$	\mathbb{I}_{19}	$-M_{16}^R L_2^R$
	$G \rightarrow I, S_2 \rightarrow M$	\mathbb{I}_{123489}	$-M_{4a}^R L_{6b(2)}^R$
	$G \rightarrow I, S_3 \rightarrow M$	$\mathbb{I}_{12456789}$	$-M_2 L_{42(2)}^R$
	$G \rightarrow I, S_1 \rightarrow I, S_2 \rightarrow M$	$\mathbb{I}_{19} \mathbb{I}_{2348}$	$+M_{4a}^R L_{4b1}^R L_2^R$
	$G \rightarrow I, S_1 \rightarrow I, S_3 \rightarrow M$	$\mathbb{I}_{19} \mathbb{I}_{245678}$	$+M_2 L_{6c(1)}^R L_2^R$
	$G \rightarrow I, S_1 \rightarrow M, S_2 \rightarrow dm$	$\mathbb{I}_{19} \mathbb{R}_{567}$	$+dm_{4a}^R M_{4b(1*)}^R L_2^R$
	$G \rightarrow I, S_3 \rightarrow M, S_2 \rightarrow dm$	$\mathbb{I}_{12489} \mathbb{R}_{567}$	$+M_2 dm_{4a}^R L_{4b2(2*)}^R$
	$G \rightarrow I, S_1 \rightarrow I, S_3 \rightarrow M, S_2 \rightarrow dm$	$\mathbb{I}_{19} \mathbb{I}_{248} \mathbb{R}_{567}$	$-M_2 dm_{4a}^R L_{2*}^R L_2^R$

Amplitude as a finite integral

- ▶ Finite amplitude ΔM_G free from both UV and IR divergences is obtained by Feynman-parameter integral as:

$$\Delta M_G = \int (dz) \left[F_G \quad \leftarrow \text{unrenormalized amplitude} \right. \\ \left. + \sum_f \prod_{S \in f} (-\mathbb{K}_S) F_G \quad \leftarrow \text{UV subtraction terms} \right. \\ \left. + \sum_{\tilde{f}} (-\mathbb{I}_{S_i}) \cdots (-\mathbb{R}_{S_j}) \cdots F_G \right] \quad \leftarrow \text{IR subtraction terms}$$

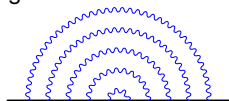
f : **Zimmermann's forests**:
combinations of UV divergent subdiagrams.

\tilde{f} : **annotated forests**:
combinations of self-energy subdiagrams
with distinction of I - R -subtractions.

Automation

- ▶ We need to evaluate a large number of Feynman diagrams. (For 10th order Set V, there are 389 independent integrals.)
- ▶ Each diagram may have large number of UV and IR subtraction parts, to each of which the subtraction integrand should be prepared.

e.g.

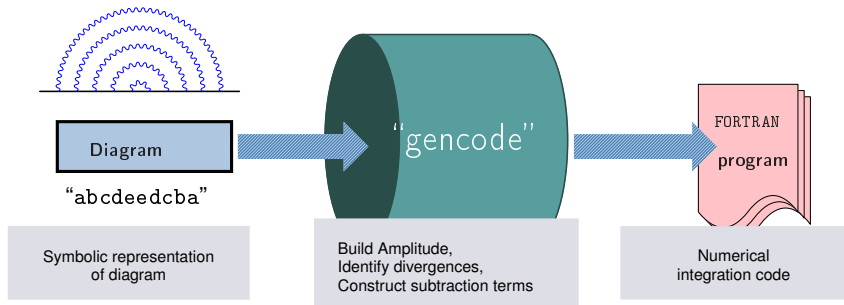


X072

15 UV-divergent parts and 119 IR-divergent parts.

- ▶ Identification of divergent parts is diagram-based, and suitable for automated treatment.
- ▶ It should be error-prone by writing numerical integration code for these huge integrals by hand. We developed an automated code-generating program.

Automation



- ▶ “gencode N ” takes a single-line information that represents a diagram, and generates numerical integration code in FORTRAN.
- ▶ “gencode N ” is tailored so that it can process any order of diagrams. This enables us to check the validity of the code generator by lower order diagrams.

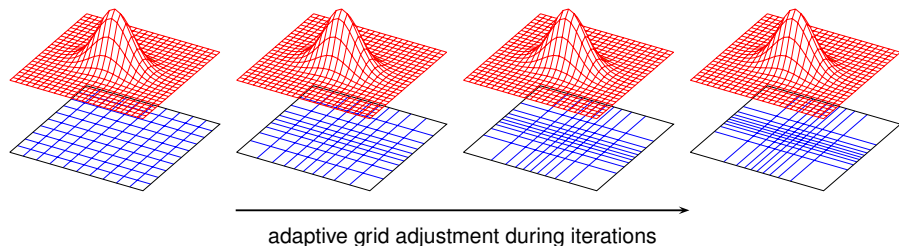
TA, Hayakawa, Kinoshita, Nio, Nucl. Phys. B 740, 138 (2006)
TA, Hayakawa, Kinoshita, Nio, Nucl. Phys. B 796, 184 (2008)

Numerical integration

- ▶ The amplitude is expressed as a multi-dimensional integral.
($D = 14 - 1$ for 10th-order diagrams)
- ▶ The integrand is a huge rational function. The size of integrand is $\mathcal{O}(10^5)$ lines of FORTRAN code per diagram.
- ▶ Numerical integration is performed by an adaptive-iterative Monte-Carlo method, VEGAS.
- ▶ Integral over D -dimensional region $I^D = [0, 1]^D$ is evaluated from N independent samples of a random variable that is distributed according to $\rho(x)$ within I^D .

Lepage, J.Comput.Phys.27, 192 (1978)

A new version of VEGAS: <https://github.com/gplepage/vegas>



Numerical precision

- ▶ Divergences are dealt with subtractive scheme point-by-point in the parameter space. Severe digit-deficiency problem may occur.
- ▶ IEEE754 double-precision floating point format:

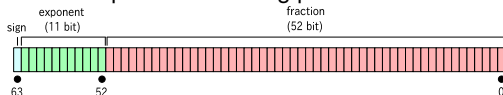
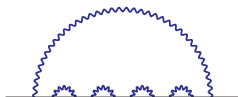


figure taken from Wikipedia

resolution is 2^{-53} (16–17 digits).

- ▶ Some diagrams with a number of self-energy subdiagrams have linear or worse IR divergences, that may exhibit unstable convergence on integration with insufficient numerical precision.
e.g.

X008



Numerical precision

- ▶ A remedy is to employ extended precision arithmetic (quadruple, etc). IEEE754 quadruple precision binary floating-point format (binary128):



figure taken from Wikipedia

This provides approximately 34 significant decimal digits.
At present, there is no hardware support in commodity facilities.

- ▶ Another option is to express a floating-point value a by a set of double-precision data

a_0, a_1, \dots as:

$$a = a_0 + \epsilon a_1 + \epsilon^2 a_2 + \dots, \quad \epsilon = 2^{-53}$$

Arithmetics over a are translated to those over a_i 's, by passing rounding-off residues to lower order components based on Knuth and Dekker algorithm.

We use “double-double” (and also “quadruple-double”) of qd library

Bailey, Hida, Li. c.f. <http://crd.lbl.gov/~dhbailey/mpdist/>

It is implemented by software, and approx. 20 times costly compared to double precision arithmetic.

Facilities

- ▶ Numerical calculations are mainly conducted on supercomputers in RIKEN.
 - ▶ RIKEN Super Combined Cluster (RSCC)
12 TFlops, Apr. 2005 – Jun. 2009
 - ▶ RIKEN Integrated Cluster of Clusters (RICC)
96 TFlops, Oct. 2009 – Mar. 2015
 - ▶ (new) RIKEN Hokusai GreatWave
1 PFlops, June. 2015 –
- ▶ Several other facilities are used e.g. workstations in Nagoya University, and KMI φ cluster computing system.



photo from RIKEN

Numerical values of Set V integrals

- ▶ Thus, the numerical evaluation of 389 integrals of Set V yields the results as follows, where each statistical uncertainty due to VEGAS Monte-Carlo integration is lower than certain criterion:

Diagram	Vertex repr.	No. of subtr. terms	Value (Error) including n_F	No. of iterations with 10^9 sampling points per iteration
X001	<i>abacbdcede</i>	47	-0.1724 (91)	20
X002 ^{dd}	<i>abaccddebe</i>	47	-5.9958 (333)	13
X003	<i>abacbdcede</i>	19	-0.1057 (52)	10
X004 ^{dd}	<i>abaccddebe</i>	71	5.1027 (339)	9
X005	<i>abacddbece</i>	43	1.1112 (168)	20
X006	<i>abaccddebe</i>	59	-5.2908 (245)	9
X007	<i>abbcadceed</i>	47	-3.4592 (254)	25
X008 ^{qd}	<i>abbccddeea</i>	47	-16.5070 (289)	11
X009	<i>abbcadceed</i>	19	-3.1069 (71)	24
X010 ^{dd}	<i>abbcddceea</i>	83	11.2644 (342)	124
X011 ^{dd}	<i>abbcddaeec</i>	43	6.0467 (338)	22
X012 ^{dd}	<i>abbcddceea</i>	67	-9.3328 (267)	26
X013	<i>abcabdecde</i>	7	-1.3710 (31)	2
X014	<i>abcacdedbe</i>	31	0.8727 (42)	10
X015	<i>abcadbecde</i>	2	2.1090 (8)	2
X016	<i>abcadcedbe</i>	2	-0.9591 (7)	2
X017	<i>abcaddebce</i>	6	0.5146 (13)	20
X018	<i>abcaddecbe</i>	6	0.0309 (13)	20
X019	<i>abcbadeced</i>	31	1.2965 (48)	10
X020 ^{dd}	<i>abcbcdedeae</i>	134	-8.1900 (318)	43
X021	<i>abcbdaeced</i>	11	-0.2948 (15)	10
X022	<i>abcbcdedeae</i>	79	0.8892 (226)	22
X023	<i>abcbddeaec</i>	27	0.4485 (55)	25
X024	<i>abcbddecea</i>	75	-6.0902 (246)	23
X025	<i>abccadeebd</i>	39	-0.7482 (194)	20
X026 ^{dd}	<i>abccbdeeda</i>	95	-7.8258 (277)	8
X027	<i>abccdaeebd</i>	15	-2.3260 (54)	13
X028 ^{dd}	<i>abccdbeeda</i>	71	4.5663 (342)	49
X029 ^{dd}	<i>abccddeab</i>	35	6.9002 (233)	1
X030 ^{dd}	<i>abccddeeba</i>	67	-12.6225 (342)	34

Residual renormalization

- ▶ We adopt the standard on-shell renormalization to ensure that the coupling constant α and the electron mass m_e are the ones measured by experiments.
- ▶ The sum of all these finite integrals defined by K-operation and I-/R-subtraction operations does not correspond to physical contribution to $g - 2$.
- ▶ The difference is adjusted by the step called the residual renormalization.

$$a_e = M(\text{bare}) - \text{on-shell renormalization}$$

$$= \underbrace{\left[M(\text{bare}) - \text{UV subtr.} - \text{IR subtr.} \right]}_{\text{Finite integral } \Delta M}$$

$$+ \underbrace{\left[-\text{on-shell renorm.} + \text{UV subtr.} + \text{IR subtr.} \right]}_{\text{finite residual renormalization}}$$

Deriving residual renormalization

- ▶ Sum up over 389 integrals of 10th order Set V, which requires analytic sum of $\sim 16,000$ symbolic terms.
- ▶ The physical contribution from 10th order Set V is thus given by:

$$\begin{aligned} A_1^{(10)}[\text{Set V}] &= \Delta M_{10}[\text{Set V}] \\ &+ \Delta M_8(-7\Delta LB_2) \\ &+ \Delta M_6\{-5\Delta LB_4 + 20(\Delta LB_2)^2\} \\ &+ \Delta M_4\{-3\Delta LB_6 + 24\Delta LB_4\Delta LB_2 - 28(\Delta LB_2)^3 + 2\Delta L_{2^*}\Delta dm_4\} \\ &+ M_2\{-\Delta LB_8 + 8\Delta LB_6\Delta LB_2 - 28\Delta LB_4(\Delta LB_2)^2 \\ &\quad + 4(\Delta LB_4)^2 + 14(\Delta LB_2)^4 + 2\Delta dm_6\Delta L_{2^*}\} \\ &+ M_2\Delta dm_4(-16\Delta L_{2^*}\Delta LB_2 + \Delta L_{4^*} - 2\Delta L_{2^*}\Delta dm_{2^*}), \end{aligned}$$

- ▶ The terms with Δ are the finite n th order quantities.
 - ▶ $\Delta M_n, M_2$: finite magnetic moment.
 - ▶ ΔLB_n : sum of vertex and wave-function renormalization constants.
 - ▶ Δdm_n : mass-renormalization constants.
 - ▶ $\Delta L_n^*, \Delta dm_n^*$: * denotes mass insertion.

Numerical evaluation of Set V

- ▶ The sum of these 389 integrals is

$$\Delta M_{10} = 3.468 \text{ (336)}$$

With the auxiliary quantities required for the residual renormalization listed below,

Integral	Value (Error)	Integral	Value (Error)
ΔM_8	1.738 12 (85)	ΔL_{4*}	-0.459 051 (62)
ΔM_6	0.425 8135 (30)	ΔL_{2*}	-0.75
ΔM_4	0.030 833 612 . . .	Δdm_6	-2.340 815 (55)
M_2	0.5	Δdm_4	1.906 3609 (90)
ΔLB_8	2.0504 (86)	Δdm_{2*}	-0.75
ΔLB_6	0.100 801 (43)		
ΔLB_4	0.027 9171 (61)		
ΔLB_2	0.75		

we obtain the 10th order contribution from Set V, $A_1^{(10)}$:

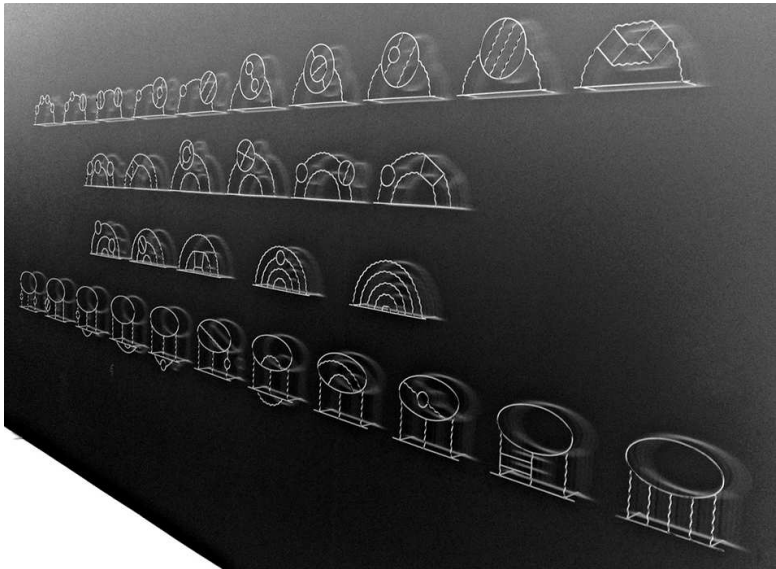
$$A_1^{(10)}[\text{Set V}] = 8.726 \text{ (336)}.$$

- ▶ Numerical evaluation of other sets are carried out in a similar manner. Next table shows the summary of these results.

Numerical values of 10th order contribution from 32 subsets

Set	n_F	universal	electron	muon		
		A_1	$A_2(m_e/m_\mu)$	$A_2(m_\mu/m_e)$	$A_2(m_\mu/m_\tau)$	$A_3(m_\mu/m_e, m_\mu/m_\tau)$
I(a)	1	0.000 470 94 (6)	0.000 000 28 (1)	22.566 973 (3)	0.000 038 (0)	0.017 312 (1)
I(b)	9	0.007 010 8 (7)	0.000 001 88 (1)	30.667 091 (3)	0.000 269 (0)	0.020 179 (1)
I(c)	9	0.023 468 (2)	0.000 002 67 (1)	5.141 395 (1)	0.000 397 (0)	0.002 330 (0)
I(d)	6	0.003 801 7 (5)	0.000 005 46 (1)	8.8921 (11)	0.000 388 (0)	0.024 487 (2)
I(e)	30	0.010 296 (4)	0.000 001 60 (1)	-0.9312 (24)	0.000 232 (0)	0.002 370 (0)
I(f)	3	0.007 568 4 (20)	0.000 047 54 (1)	3.685 049 (90)	0.002 162 (0)	0.023 390 (2)
I(g)	9	0.028 569 (6)	0.000 024 45 (1)	2.607 87 (72)	0.001 698 (0)	0.002 729 (1)
I(h)	30	0.001 696 (13)	-0.000 010 14 (3)	-0.5686 (11)	0.000 163 (1)	0.001 976 (3)
I(i)	105	0.017 47 (11)	0.000 001 67 (2)	0.0871 (59)	0.000 024 (0)	0
I(j)	6	0.000 397 5 (18)	0.000 002 41 (6)	-1.263 72 (14)	0.000 168 (1)	0.000 110 (5)
II(a)	24	-0.109 495 (23)	-0.000 737 69 (95)	-70.4717 (38)	-0.018 882 (8)	-0.290 853 (85)
II(b)	108	-0.473 559 (84)	-0.000 645 62 (95)	-34.7715 (26)	-0.035 615 (20)	-0.127 369 (60)
II(c)	36	-0.116 489 (32)	-0.000 380 25 (46)	-5.385 75 (99)	-0.016 348 (14)	-0.040 800 (51)
II(d)	180	-0.243 00 (29)	-0.000 098 17 (41)	0.4972 (65)	-0.007 673 (14)	0
II(e)	180	-1.344 9 (10)	-0.000 465 0 (40)	3.265 (12)	-0.038 06 (13)	0
II(f)	72	-2.433 6 (15)	-0.005 868 (39)	-77.465 (12)	-0.267 23 (73)	-0.502 95 (68)
III(a)	300	2.127 33 (17)	0.007 511 (11)	109.116 (33)	0.283 000 (32)	0.891 40 (44)
III(b)	450	3.327 12 (45)	0.002 794 (1)	11.9367 (45)	0.143 600 (10)	0
III(c)	390	4.921 (11)	0.003 70 (36)	7.37 (15)	0.1999 (28)	0
IV	2072	-7.7296 (48)	-0.011 36 (7)	-38.79 (17)	-0.4357 (25)	0
V	6354	8.726 (336)	0	0	0	0
VI(a)	36	1.041 32 (19)	0.006 152 (11)	629.141 (12)	0.246 10 (18)	2.3590 (18)
VI(b)	54	1.346 99 (28)	0.001 778 9 (35)	181.1285 (51)	0.096 522 (93)	0.194 76 (26)
VI(c)	144	-2.5289 (28)	-0.005 953 (59)	-36.58 (12)	-0.2601 (28)	-0.5018 (89)
VI(d)	492	1.8467 (70)	0.001 276 (76)	-7.92 (60)	0.0818 (17)	0
VI(e)	48	-0.4312 (7)	-0.000 750 (8)	-4.32 (14)	-0.035 94 (32)	-0.1122 (24)
VI(f)	180	0.7703 (22)	0.000 033 (7)	-38.16 (15)	0.043 47 (85)	0.0659 (31)
VI(g)	480	-1.5904 (63)	-0.000 497 (29)	6.96 (48)	-0.044 51 (96)	0
VI(h)	630	0.1792 (39)	0.000 045 (9)	-8.55 (23)	0.004 85 (46)	0
VI(i)	60	-0.0438 (12)	-0.000 326 (1)	-27.34 (12)	-0.003 45 (33)	-0.0027 (11)
VI(j)	54	-0.2288 (18)	-0.000 127 (13)	-25.505 (20)	-0.011 49 (33)	-0.016 03 (58)
VI(k)	120	0.6802 (38)	0.000 015 6 (40)	97.123 (62)	0.002 17 (16)	0
sum	12672	7.795 (336)	-0.003 82 (39)	742.18 (87)	-0.068 (5)	2.011 (10)

Summary and discussion



Feynman diagrams exhibited at Fermilab Art Gallery by Edward Tufte
Photo from *The Work of Edward Tufte and Graphics Press*

Summary and discussion

- ▶ For the electron $g-2$, the experimental precision has reached to 0.24 ppb, while the perturbative contribution of QED up to 10th order $(\alpha/\pi)^5$ has now been available. The experiment and the theory of a_e agrees to $O(10^{-12})$.
- ▶ From $a_e(\text{exp})$ and $a_e(\text{theory})$, the most precise determination of the fine structure constant α is obtained, with the precision of 0.25 ppb.
- ▶ New measurement is being prepared with new apparatus for the positron $g-2$ by the Harvard group. Further improvement on the experiment is expected.
- ▶ The largest source of theoretical uncertainty at present is the 8th order QED term. Improvement on the numerical evaluation of 8th term as well as 10th order term is continuously in progress.
- ▶ Improvement on the non-QED α is crucial as the input of the theoretical prediction. Comparison of α from different determinations provides another stringent test of QED.

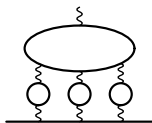
Summary and discussion

- ▶ For the muon $g-2$, the discrepancy between the experiment and the theory is being observed by 2.7σ . It is an urgent problem to understand whether it persists or not with the improvement of both experiment and theory.
- ▶ New experiments are being prepared at Fermilab and J-PARC, both aiming at 0.1 ppm level.
- ▶ The QED contribution is dominant but it has been known precisely enough for the next experiments, with the complete evaluation of the 10th order term. We can now concentrate on the hadronic contribution, the present largest source of theoretical uncertainty by 0.6ppm.
- ▶ Lattice QCD will be a promising tool for the evaluation of the hadronic contribution.

This will be the subject of the next speaker, Izubuchi-san, and of a number of parallel talks in this conference.

Summary and discussion

- ▶ *Do we need 6-loop contribution?*
- ▶ There are 202,770 vertex Feynman diagrams contributing to 12th order. The Feynman-parametric integral involves 16 dimensional numerical integration, each combinatorially more complicated than those of 10th order.
- ▶ Consider that $\left(\frac{\alpha}{\pi}\right)^6 \sim O(10^{-16})$, and the present uncertainty of a_e is of $O(10^{-13})$, it is not likely that 12th-order contribution is needed for the time being.
- ▶ For the muon $g-2$, a large numerical factor is expected from the electron loops. The leading contribution will come from three insertions of 2nd-order vacuum-polarization loop into the 6th-order light-by-light diagram. It is estimated as:



$$\sim A_2^{(6)}(m_\mu/m_e; \text{l-by-l}) \times \left\{ \frac{2}{3} \ln \left(\frac{m_\mu}{m_e} \right) - \frac{5}{9} \right\}^3 \times 10 \times \left(\frac{\alpha}{\pi} \right)^6$$
$$\sim 0.08 \times 10^{-11}.$$

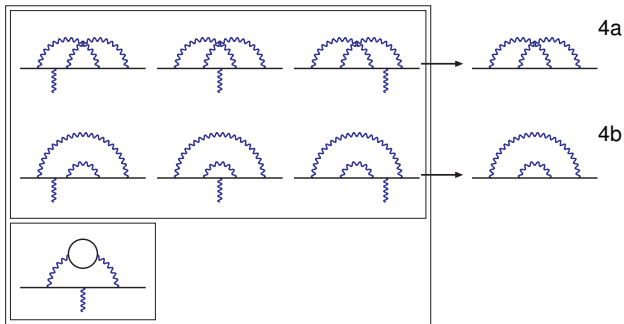
It is larger than the uncertainty of 10th order term. A crude evaluation may be desirable.

Thank you.

Backup

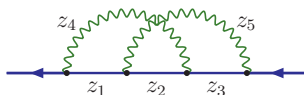
Step-by-step example with 4th-order diagrams

- ▶ Let us illustrate the steps by simpler case, e.g. 4th-order diagrams.
- ▶ There are 7 diagrams of 4th order; 6 of them have no closed lepton loop (q-type).
- ▶ They are *WT-summed* into 2 self-energy-like diagrams, 4a and 4b.



Step 1: Amplitude

- Introduce Feynman parameters z_1, \dots, z_5 to propagators:



- Anomalous magnetic moment M_{4a} is converted analytically into the form:

$$M_{4a} = \int (dz) \mathcal{F}_{4a} = \int (dz) \left[\frac{E_0 + C_0}{U^2 V} + \frac{N_0 + Z_0}{U^2 V^2} + \frac{N_1 + Z_1}{U^3 V} \right]$$

where integrand and building blocks are given as follows:

$$(dz) = dz_1 dz_2 dz_3 dz_4 dz_5 \delta(1 - z_{12345})$$

$$B_{11} = z_{235}, B_{12} = z_{35}, B_{13} = -z_2,$$

$$B_{23} = z_{14}, B_{22} = z_{1345}, B_{33} = z_{124},$$

$$U = z_2 B_{12} + z_{14} B_{11},$$

$$A_i = 1 - (z_1 B_{1i} + z_2 B_{2i} + z_3 B_{3i}) / U,$$

$$G = z_1 A_1 + z_2 A_2 + z_3 A_3, V = z_{123} - G,$$

$$z_{ijk\dots} = z_i + z_j + z_k + \dots$$

$$E_0 = 8(2A_1 A_2 A_3 - A_1 A_2 - A_1 A_3 - A_2 A_3)$$

$$C_0 = -24Z_4 Z_5 / U$$

$$N_0 = G(E_0 - 8(2A_2 - 1))$$

$$Z_0 = 8z_1(-A_1 + A_2 + A_3 + A_1 A_2 + A_1 A_3 - A_2 A_3)$$

$$+ 8z_2(1 - A_1 A_2 + A_1 A_3 - A_2 A_3 + 2A_1 A_2 A_3)$$

$$+ 8z_3(A_1 + A_2 - A_3 - A_1 A_2 + A_1 A_3 + A_2 A_3)$$

$$N_1 = 8G(B_{12}(2 - A_3) + 2B_{13}(1 - 2A_2) + B_{23}(2 - A_1))$$

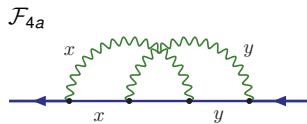
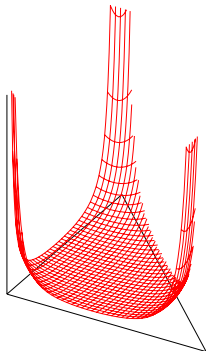
$$Z_1 = -8z_1(B_{12}(1 - A_3) + B_{13} + B_{23}A_1)$$

$$+ 8z_2(B_{12}(1 - A_3) - 4B_{13}A_2 + B_{23}(1 - A_1))$$

$$- 8z_3(B_{12}A_3 + B_{13} + B_{23}(1 - A_1))$$

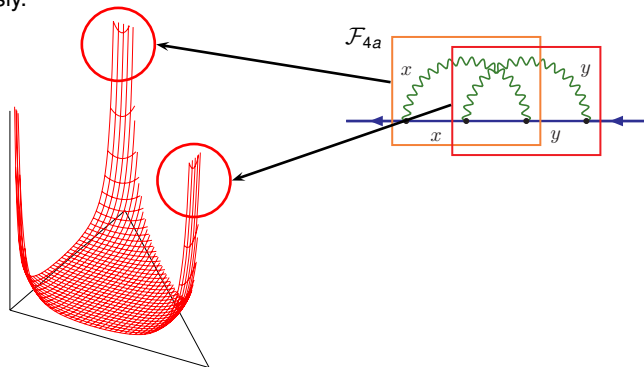
Step 2: UV subtraction

- ▶ M_{4a} is not well-defined — it has UV divergences when the loop momenta goes to infinity.



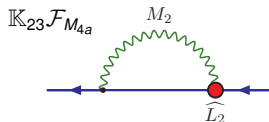
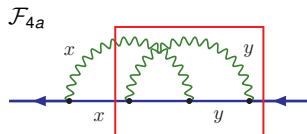
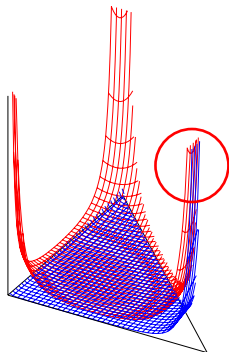
Step 2: UV subtraction

- ▶ M_{4a} is not well-defined — it has UV divergences when the loop momenta goes to infinity.
- ▶ This corresponds to a region of z_i 's when all z_i on the loop vanish simultaneously.



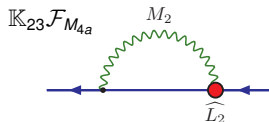
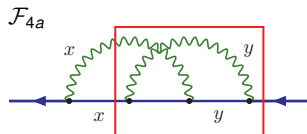
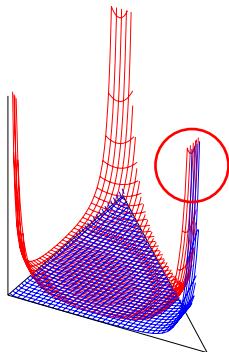
Step 2: UV subtraction

- ▶ We prepare an integral which has the same UV divergent profile by K -operation, and perform subtraction point-by-point on the integrand.



Step 2: UV subtraction

- ▶ We prepare an integral which has the same UV divergent profile by K -operation, and perform subtraction point-by-point on the integrand.



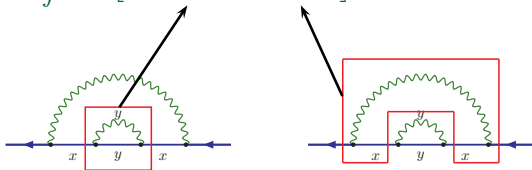
- ▶ Then the finite part of the anomalous magnetic moment ΔM_{4a} is obtained by the integral:

$$\Delta M_{4a} = \int (dz) \left[\mathcal{F}_{4a} - \mathbb{K}_{12} \mathcal{F}_{4a} - \mathbb{K}_{23} \mathcal{F}_{4a} \right]$$

Step 3: IR subtraction

- ▶ M_{4b} has IR divergence as well, from vanishing of virtual photon momentum.
- ▶ This logarithmic IR divergence is handled by an integral which is constructed by I -subtraction.
- ▶ Then the finite part of the anomalous magnetic moment ΔM_{4b} is obtained by the integral:

$$\Delta M_{4b} = \int (dz) \left[\mathcal{F}_{4b} - \mathbb{K}_{22} \mathcal{F}_{4b} - \mathbb{I}_{13} \mathcal{F}_{4b} \right]$$



Step 4: Residual renormalization

- ▶ Finite part of amplitude is given in terms of integral with appropriate UV and/or IR subtraction terms.

$$\Delta M_{4a} = \int (dz) \left[\mathcal{F}_{4a} - \mathbb{K}_{12} \mathcal{F}_{4a} - \mathbb{K}_{23} \mathcal{F}_{4a} \right]$$

$$\Delta M_{4b} = \int (dz) \left[\mathcal{F}_{4b} - \mathbb{K}_{22} \mathcal{F}_{4b} - \mathbb{I}_{13} \mathcal{F}_{4b} \right]$$

Step 4: Residual renormalization

- ▶ Finite part of amplitude is given in terms of integral with appropriate UV and/or IR subtraction terms.

$$\begin{aligned}\Delta M_{4a} &= \int (dz) \left[\mathcal{F}_{4a} - \mathbb{K}_{12} \mathcal{F}_{4a} - \mathbb{K}_{23} \mathcal{F}_{4a} \right] \\ &= M_{4a} - \widehat{L}_2 M_2 - \widehat{L}_2 M_2\end{aligned}$$

$$\begin{aligned}\Delta M_{4b} &= \int (dz) \left[\mathcal{F}_{4b} - \mathbb{K}_{22} \mathcal{F}_{4b} - \mathbb{I}_{13} \mathcal{F}_{4b} \right] \\ &= M_{4b} - (\delta m_2 M_{2^*} + \widehat{B}_2 M_2) - \widetilde{L}_2 M_2\end{aligned}$$

- ▶ Subtraction terms are analytically factorized into products of lower-order quantities.

Step 4: Residual renormalization

- ▶ Finite part of amplitude is given in terms of integral with appropriate UV and/or IR subtraction terms.

$$\begin{aligned}\Delta M_{4a} &= \int (dz) \left[\mathcal{F}_{4a} - \mathbb{K}_{12} \mathcal{F}_{4a} - \mathbb{K}_{23} \mathcal{F}_{4a} \right] \\ &= M_{4a} - \widehat{L}_2 M_2 - \widehat{L}_2 M_2\end{aligned}$$

$$\begin{aligned}\Delta M_{4b} &= \int (dz) \left[\mathcal{F}_{4b} - \mathbb{K}_{22} \mathcal{F}_{4b} - \mathbb{I}_{13} \mathcal{F}_{4b} \right] \\ &= M_{4b} - (\delta m_2 M_{2^*} + \widehat{B}_2 M_2) - \widetilde{L}_2 M_2\end{aligned}$$

- ▶ Subtraction terms are analytically factorized into products of lower-order quantities.
- ▶ Standard on-shell renormalization is denoted by

$$\begin{aligned}a^{(4)}[\text{q-type}] &= M_{4a} - 2L_2 M_2 \\ &\quad + M_{4b} - (\delta m_2 M_{2^*} + B_2 M_2)\end{aligned}$$

- ▶ By substitution, magnetic moment is given

$$a^{(4)}[\text{q-type}] = (\Delta M_{4a} + \Delta M_{4b}) - \Delta L B_2 M_2$$

where $\Delta L B_2$ is finite part of $L_2 + B_2$.